

Carbon Nanotubes Synthesis by Chemical Vapor Deposition of Methane over Zn – Fe Mixed Catalysts Supported on Alumina

Alireza Badii*, Mazaher Azmard, Mahdi Karimi, Pezhman Zarabadi-poor

School of Chemistry, College of Science, University of Tehran, Tehran, Iran

Article history:

Received 7/7/2014

Accepted 13/8/2014

Published online 1/9/2014

Keywords:

Carbon nanotube

Chemical vapor deposition

Zn-Fe/alumina catalyst

Methane

*Corresponding author:

E-mail address:

abadiei@khayam.ut.ac.ir

Phone: +98 21 61112614

Fax: +98 21 66405141

Abstract

Carbon nanotubes were synthesized over a series of Zn-containing Fe/alumina catalysts by chemical vapor deposition method at two reaction temperatures of 850 and 950 °C using methane as a carbon source. Catalysts were synthesized by keeping Fe concentration constant and varying Zn concentration to study the effects of Zn. The catalysts were characterized using X – ray powder diffraction and N₂ adsorption – desorption methods which confirmed the successful synthesis of catalysts and metals particles were inserted in alumina pores. The synthesized Carbon nanotubes were tested by scanning electron microscopy (SEM), transmission electron microscopy (TEM), thermogravimetry analysis (TGA) and Raman spectroscopy. SEM images showed that the diameter of nanotubes almost was decreased with increasing Zn content of catalysts. In Raman spectroscopy, two main bands related to the carbon nanotubes were observed. Further, TGA results revealed that the percent of synthesized carbon nanotubes were almost increased with increasing [Zn]/[Fe] proportions.

2014 JNS All rights reserved

1. Introduction

since the first report of Ijima on the synthesis of carbon nanotube (CNT)[1] came out, the catalytic chemical vapor deposition (CCVD) has become the most commonly used method for producing CNTs[2-4]. This method involves decomposition of carbon contained molecules and diffusion of formed carbon species into the catalyst particles which results in the

growth of CNTs. Various parameters control the CCVD process, including type and composition of catalyst, reaction temperature, gas flow rate and carbon source[5]. Although many researches dedicated to evaluate the influences of those above mentioned parameters, finding the optimal conditions still needs to be investigated more[6-9].

The catalyst plays crucial role in the CVD process, because it provides sites for growing CNTs and determines the diameter and yield of CNTs[10]. So far, various transition metals have been examined as a catalyst[11]. In addition, in order to make catalysts more efficient, the combination of transition metals - Fe/Co[12], Co/Ni[13], Fe/Ni[14], Fe/Cr[15], Co/Mo[16] - have been frequently evaluated. The effects of reaction temperature have also been the focus of many studies[6, 17-19]. The higher temperature is frequently reported that it gives better results in the terms of both quality and quantity of produced CNTs[19], but the lower temperatures is also reported to be effective more than higher one[17].

At our lab, the effects a series of Fe/alumina catalysts were studied[20] and in continuation of their work, it was decided that the effects of insertion of Zn on Fe/alumina function and reaction temperature be evaluated. Therefore, a series of Zn-contained Fe/alumina catalysts with constant Fe and different Zn concentrations were prepared. In this work, methane was used as a carbon source, because it was reported that methane produced least carbon byproduct[21]. To uniformly distribute and to prevent the aggregation of metal particles, the use of support, which strongly bonded to metal particles and provided large specific area, is needed. Alumina well qualifies those mentioned requirements, hence, it was used as a catalyst support.

2. Experimental

2.1. Materials

The chemicals, including $\text{Fe}(\text{NO}_3)_3 \cdot 9\text{H}_2\text{O}$ (Merck), $\text{Zn}(\text{NO}_3)_2 \cdot 4\text{H}_2\text{O}$ (Merck) methanol (Merck), Methane (99.99%), Alumina (Jajarm-Iran, specific surface area : $55 \text{ m}^2/\text{g}$ and pore diameter: 9 nm) were all of analytical reagent grade and used without further treatment.

2.2. Preparation of the catalysts

Catalysts were prepared based on ref.[20] An appropriate amount of Fe and Zn nitrate salts were dissolved in methanol for preparing $\text{Fe}(\text{NO}_3)_3 \cdot 9\text{H}_2\text{O}$ 0.05 M and $\text{Zn}(\text{NO}_3)_2 \cdot 4\text{H}_2\text{O}$ X M (where X: 0.0125, 0.025, 0.05, 0.1, 0.2 M). Then, 15 ml of $\text{Fe}(\text{NO}_3)_3 \cdot 9\text{H}_2\text{O}$ 0.05 M and 15 ml of $\text{Zn}(\text{NO}_3)_2 \cdot 4\text{H}_2\text{O}$ X M were simultaneously mixed with 1 g alumina and stirred for 1.5 h at room temperature. Then, methanol was removed by a rotary evaporator. Finally, the prepared solids were dried overnight at $150 \text{ }^\circ\text{C}$ and grounded in fine powder by a mortar and pestle. Table 1 lists the prepared catalysts.

Table 1. The list of prepared catalysts

catalyst code	[Zn] mol.L ⁻¹	[Fe] mol.L ⁻¹	[Zn]/[Fe]	S _{BET} m ² .g ⁻¹	Pore volume ml.g ⁻¹
Zn ₄ Fe	0.2	0.05	4	17	0.08
Zn ₂ Fe	0.1	0.05	2	30	0.1
Zn ₁ Fe	0.05	0.05	1	35	0.14
Zn _{0.5} Fe	0.025	0.05	0.5	40	0.17
Zn _{0.25} Fe	0.0125	0.05	0.25	49	0.18

2.3. Carbon nanotubes synthesis

The synthesis procedure was done based on ref.[20] with slight modifications. Typically, 0.3 g of catalyst powder was putted into a boat crucible which inserted into a quartz tube. Then, crucible located in furnace and heated up to desired temperature (in this case, 850 and 950 °C) while argon gas was flowed into the tube to eliminate the oxygen in reaction ambient. Once the desired temperature was reached, the gas flow was switched to the methane for 1h. Finally, the furnace was slowly cooled down to room temperature while the flow was again turned back to

the argon. Hereafter, we refer to synthesized CNTs as Zn_xCNT_y where X represents the proportion of $[Zn]/[Fe]$ and Y represents the reaction temperature.

2.4. Characterization methods

N_2 adsorption–desorption isotherms were measured using BELSORP-miniII at liquid nitrogen temperature (77 K). All samples were degassed at 300 °C for 3 h under inert gas flow prior to perform analyses. The specific surface area were evaluated using the Brunauer–Emmett–Teller (BET) method. X-ray powder diffraction (XRD) patterns were obtained on a Philips X'PERT diffractometer using Cu K α radiation 40 kV and 40 mA. Scanning electron microscopy (SEM) was carried out on a LEO 1445V microscope. Transmission electron microscopy (TEM) was performed on a 90 kV Philips EM208 under an accelerated voltage of 100 kV. Samples were dispersed in ethanol using an ultrasonic bath, and a drop placed on a lacey carboncoated copper grid for analysis. Thermogravimetric analysis (TGA) was carried out in NIETZSCH STA 409 PC/GP instrument from ambient temperature to 1000 °C, using a ramp rate of 10 °C/min. Micro-Raman spectra were recorded using a SENTERRA - Bruker spectrometer, equipped with 3 lasers (785, 633 and 532 nm), a 20 mW Nd:YAg Laser, and CCD (1024 x 128 pixels) detector.

3. Results and discussions

3.1. Catalyst characterization

Figure 1A shows N_2 adsorption – desorption isotherm of the catalysts and alumina. The alumina belongs to the mesoporous materials with type IV standard isotherm (Figure 1A(a))[20]. As it can be

seen, the hysteresis loops in all the catalysts resemble the alumina one which indicates that they preserved original mesoporous structure of alumina during impregnation process. Moreover, the decrease in the height of isotherms with the increasing of the zinc concentration implied that more metal particles were inserted into the alumina pores, which led to the decrease in the accessible pore volume for N_2 adsorption - desorption. This explanation is supported by the pore volume data of the catalysts as it's shown in the table1.

Figure 1B gives the BJH pore diameter distributions of the catalysts. The BJH of alumina shows two main pore diameter distribution peaks which are located almost at $r_p = 4$ and 7 nm. With increasing of the zinc concentrations, the more particles were put into the pores, the more the height of this two peaks decreased. Although the short peak around $r_p = 3$ nm remained nearly unchanged. It can be assumed that catalyst particles are inserted into and filled the pore with larger diameters. decreased. Although the short peak around $r_p = 3$ nm remained nearly unchanged. It can be assumed that catalyst particles are inserted into and filled the pore with larger diameters.

The XRD patterns of alumina and catalysts are depicted in the Fig.2. The alumina peaks were observed in all the catalyst patterns, although they dropped sharply. Also, the new peaks related to the presence of zinc and iron metals didn't observe. It can be suggested that due to being in smaller amount with respect to the amount of alumina, Zn and Fe related peaks can't be observed. Moreover, metal particles substitute into the alumina lattice to a small extent which results in the decrease of lattice plane reflection and intensity.

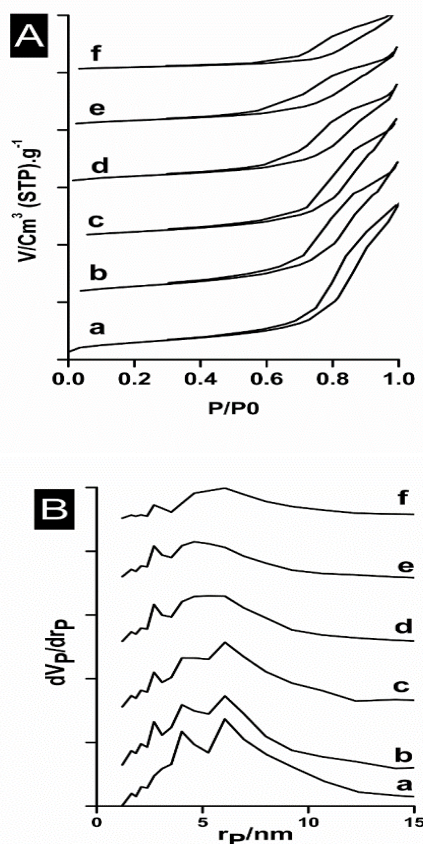


Fig. 1. (A) N_2 adsorption – desorption and (B) BJH pore diameter distribution of (a) Alumina, (b) $Zn_{0.25}Fe$, (c) $Zn_{0.5}Fe$, (d) Zn_1Fe , (e) Zn_2Fe and (f) Zn_4Fe .

3.2. Carbon nanotube characterizations

Figures 3 and 4 give the SEM images of resulted CNTs at the reaction temperatures of 850 and 950 °C, respectively. As it can be observed, all the samples contained CNTs, however more amount of CNTs was observed at the reaction temperature of 950 °C than 850°C comparatively. Also, the external morphology of CNTs depended on both the temperature and the Zn content of the catalysts.

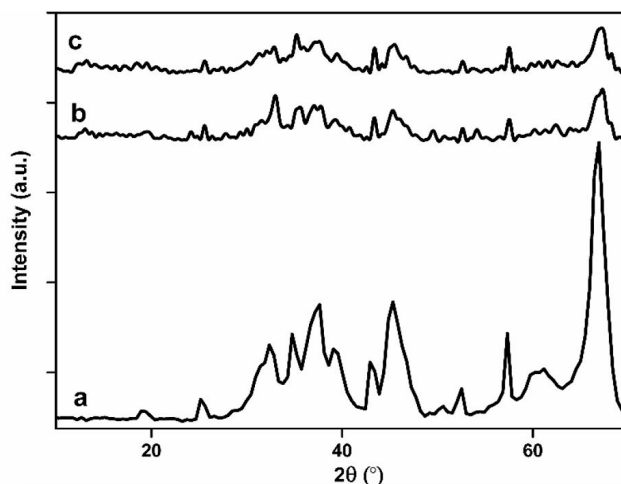


Fig. 2. XRD patterns of (a) alumina, (b) Zn_4Fe , (c) Zn_2Fe .

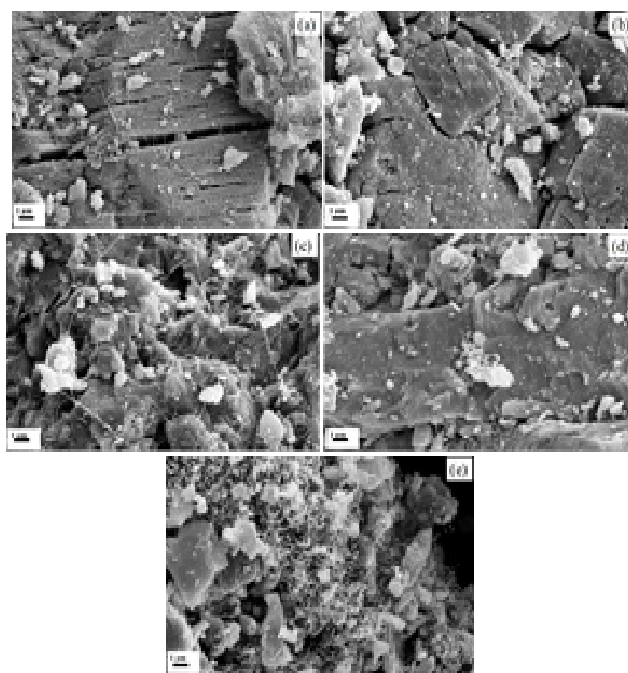


Fig. 3. SEM images of (a) Zn_4NT_{850} , (b) Zn_4NT_{850} , (c) Zn_1NT_{850} , (d) $Zn_{0.5}NT_{850}$ (e) $Zn_{0.25}NT_{850}$.

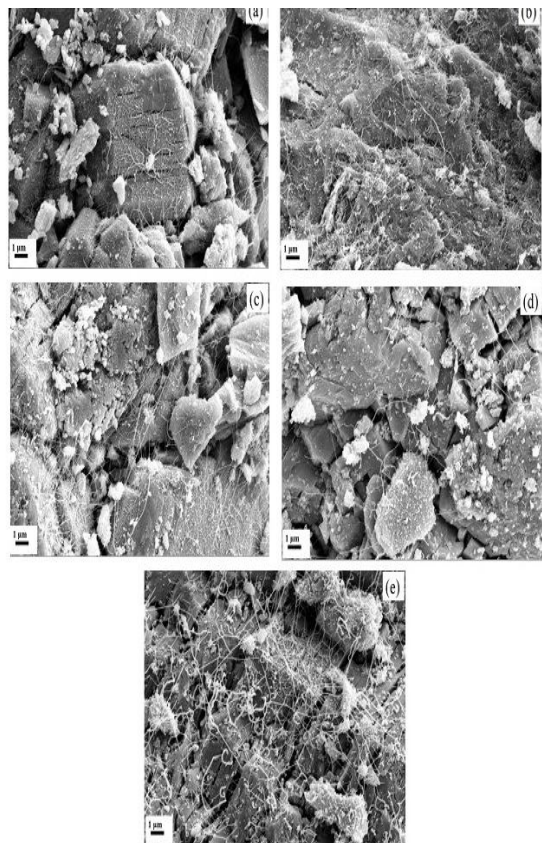


Fig. 4. SEM images of (a) Zn_4NT_{950} , (b) Zn_2NT_{950} , (c) Zn_1NT_{950} , (d) $Zn_{0.5}NT_{950}$ and (e) $Zn_{0.25}NT_{950}$.

Figure 5 provides the measured diameter distributions of CNTs corresponds to the SEM images in Figures 3 and 4. Based on this diagram, with increasing of the temperature and Zn concentration, the CNT diameters were decreased. This phenomena could be explained by vapor – liquid – solid (VLS) theory[10]. Based on this theory, the diameter of catalyst particles control the diameter of resulted CNTs. Therefore, the decreasing of CNT diameters was resulted from catalyst particle decreasing. Thus, it can be proposed that the increasing of Zn concentration prevented catalyst particle agglomerations and hence decreased catalyst particle sizes.

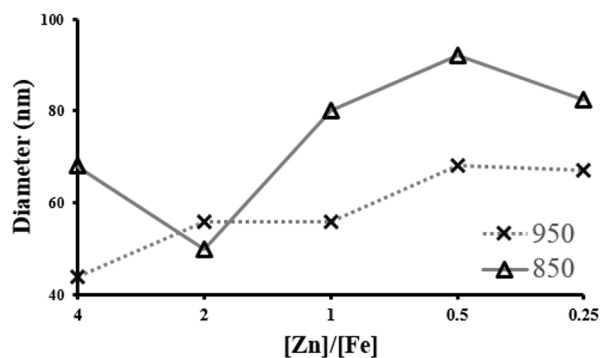


Fig. 5. Diagram of Average diameters of resulted carbon nanotubes using catalysts with the $[Zn]/[Fe]$ proportion of 4, 2, 1, 0.5 and 0.25 at reaction temperatures of 850 and 950 °C.

TEM images of $Zn_{0.05}NT_{950}$ is typically given in Figure 6. The observation of hollow tube with an outer diameter about 50 nm confirmed that carbon nanotubes were synthesized out of the other carbon forms. Also, the small dark particle with diameter about 45 nm inside the carbon nanotubes has almost the same diameter of some synthesized CNTs.

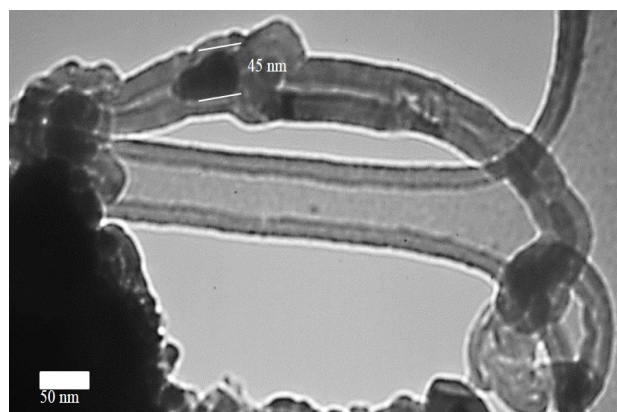


Fig. 6. TEM images of $Zn_{0.5}CNT_{950}$.

Figure 7 shows the TGA curves of as-synthesized $Zn_{0.1}NT$. Weight loss between 25 to 400 °C is related to the elimination of absorbed water and amorphous carbon and above 400 °C is attributed to the CNT losses[22, 23]. From Small weight loss between 25 to 400 °C, it can be inferred that the use of methane as a carbon source didn't result in the production of amorphous carbon.

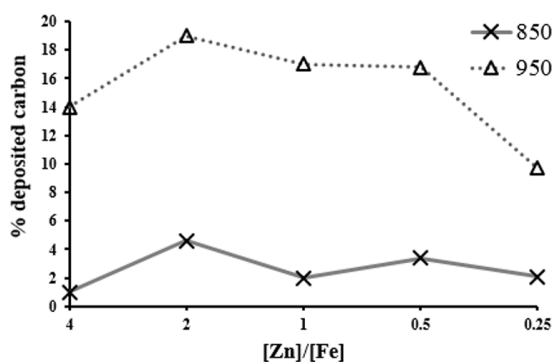


Fig. 8. Diagram of the weight loss percent of resulted carbon nanotubes using catalysts with the $[Zn]/[Fe]$ proportion of 4, 2, 1, 0.5 and 0.25 at reaction temperatures of 850 and 950 °C.

Figure 8 provides the diagram of the measured percent of the deposited carbon nanotubes. As it can be drawn, the percent of the produced CNTs at 950 °C is nearly five times larger than that of 850°. It can be suggested that the higher reaction temperature of 950 °C provided more thermal energy for methane decomposition, and therefore, more produced C_n species consequently became available. Then, the more catalyst particles get involved in growing carbon nanotubes. Further, the increasing of Zn concentration to 0.1 M gave rise to the increasing of the yield of CNTs. This increase can be due to the insertion of additional active sites for CNT growth. Raman spectra of $Zn_{0.05}NT$ for both reaction temperatures of 850 and 950 °C are given in the Figure 9. Both of samples show two major peaks

around 1350 cm^{-1} (D-band) and 1600 cm^{-1} (G-band). In general, D-band represents the existence of amorphous carbon or defect in the wall of CNTs and G-band represents the degree of crystallinity in the graphite structure of CNT[24, 25]. The presence of D-band and G-band together suggested that multiwall carbon nanotubes were synthesized. Furthermore, synthesized $Zn_{0.05}NT$ at 950 °C had a higher G-band than that of 850 °C which indicates that obtained CNTs at 950 °C have the better quality of synthesized CNTs at 850 °C.

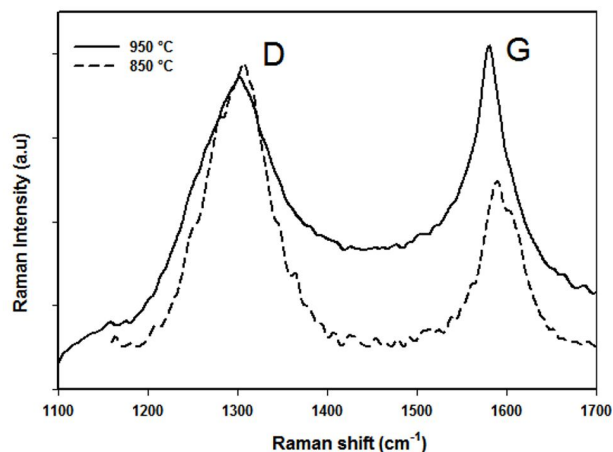


Fig. 9. Typical Raman spectra of Zn_2CNT_{950} and Zn_2CNT_{850} .

4. Conclusion

In conclusion, carbon nanotubes were synthesized by catalytic chemical vapor deposition of methane over Zn-containing Fe/alumina catalysts at two reaction temperatures of 850 and 950 °C. N_2 adsorption – desorption and XRD analysis were used to characterization of catalysts. These analyses showed that the basic structure of support was not altered after loading metals particles and catalyst particles were inserted into the alumina pores. SEM and TEM microscopy, Raman spectroscopy and TGA analysis were used to study synthesized CNTs. SEM, TEM and Raman approved the presence of CNTs. It

was found that with increasing of the Zn content of catalysts and reaction temperature, the percent of deposited CNTs was approximately increased. The higher percent was achieved by using of Zn₂Fe catalyst at 950 °C. Moreover, the diameter of produced CNTs showed the dependence on the Zn content, that is, the diameters were almost decreased with the increase in Zn content. Regarding Raman spectra and the diameter of CNT in TEM image, multiwall carbon nanotubes were more likely obtained.

References

- [1] S. Iijima, *nature*. 354 (1991) 56-58.
- [2] M.L. Terranova, V. Sessa, M. Rossi, *Chem. Vap. Deposition*. 12 (2006) 315-325.
- [3] A. Magrez, J.W. Seo, R. Smajda, M. Mionić, L. Forró, *Materials*. 3 (2010) 4871-4891.
- [4] V. Jourdain, C. Bichara, *Carbon*. 58 (2013) 2-39.
- [5] Ç. Öncel, Y. Yürüm, *Fuller. Nanotub. CarbonNanostruct*. 14 (2006) 17-37.
- [6] X. Fu, X. Cui, X. Wei, J. Ma, *App. Surf. Sci*. 292 (2014) 645-649.
- [7] F. Taleshi, *Fuller. Nanotub. CarbonNanostruct*. 22 (2014) 921-927.
- [8] S. Pooperasupong, B. Caussat, P. Serp, S. Damronglerd, *J. Chem. Eng. Jpn*. 47 (2014) 28-39.
- [9] R. Xie, G. Zhong, C. Zhang, B. Chen, C.S. Esconjauregui, J. Robertson, *J. App. Phys*. 114 (2013) 244-302.
- [10] S.B. Sinnott, R. Andrews, D. Qian, A.M. Rao, Z. Mao, E.C. Dickey, F. Derbyshire, *Chem. Phys. Lett*. 315 (1999) 25-30.
- [11] W. Zhou, L. Ding, Liu, *J Nano Res*. 2 (2009) 593-598.
- [12] J. Wen, W. Chu, C. Jiang, D. Tong, *J. Nat. Gas Chem*. 19 (2010) 156-160.
- [13] D.L. Cursaru, D. Enescu, D. Ciuparu, *Rev. Chim*. 62 (2011) 792-798.
- [14] H. Patel, L.M. Manocha, S. Manocha, *Nano. Nanotechol- Asia*. 2 (2012) 66-75.
- [15] M.A. Pasha, A. Shafiekhani, M.A. Vesaghi, *Appl. Surf. Sci*. 256 (2009) 1365-1371.
- [16] W.M. Yeoh, K.Y. Lee, S.P. Chai, K.T. Lee, A.R. Mohamed, *J. Phys. Chem. Solids*. 74 (2013) 1553-1559.
- [17] N. Arnaiz, M.F. Gomez-Rico, I. Martin Gullon, R. Font, *Ind. Eng. Chem. Res*. 52 (2013) 14847-14854.
- [18] S.L. Pirard, A. Delafosse, D. Toye, J.P. Pirard, *Chem. Eng. J*. 232 (2013) 488-494.
- [19] S. Taş, F. Okyay, M. Sezen, H. Plank, Y. Yürüm, *Fuller. Nanotub. CarbonNanostruct*. 21 (2013) 311-325.
- [20] P. Zarabadi-Poor, A. Badiei, A. Yousefi, B. Fahlman, A. Abbasi, *Cata. Today*. 150 (2010) 100-106.
- [21] J. Kong, A.M. Cassell, H.Dai, *Chem. Phys. Lett*. 292 (1998) 567-574.
- [22] I. Abdullahi, N. Sakulchaicharoen, J.E. Herrera, *Diamond Relat. Mater*. 41 (2014) 84-93.
- [23] S. Lim, N. Li, F. Fang, M. Pinault, C. Zoican, C. Wang, T. Fadel, L.D. Pfefferle, G.L. Haller, *J. Phys. Chem. C*. 112 (2008) 12442-12454.
- [24] M.S. Dresselhaus, G. Dresselhaus, A. Jorio, A.G. Souza Filho, R. Saito, *Carbon*. 40 (2002) 2043-2061.
- [25] L. Lafi, D. Cossement, R. Chahine, *Carbon*. 43 (2005) 1347-1357.